An Integrated Method to Rectify Airborne Radar Imagery Using DEM

Thierry Toutin
Canada Centre for Remote Sensing, 2464 Sheffield Road, Ottawa, Ontario K1A 0Y7, Canada
*Yves Carbonneau**
Prologic Systems Ltd., 75 Albert Street, Suite 206, Ottawa, Ontario K1P 5E7, Canada
Louiselle St-Laurent
Canada Centre for Remote Sensing, 2464 Sheffield Road, Ottawa, Ontario K1A 0Y7, Canada

ABSTRACT: A fully digital procedure to geometrically correct airborne synthetic aperture radar (SAR) data is described; it uses an integrated geometric correction model to remove distortions produced by viewing geometry, including terrain-induced effects. This model, originally developed to process digital SPOT data, is extended to the case of SAR data. For the airborne SAR example studied, geometric corrections achieved an accuracy of 10 to 12 metres, e.g., about two pixels of the SAR image used, with 8 to 10 ground control points (GCPs).

INTRODUCTION

THEMATIC APPLICATIONS, AS IN HYDROLOGY, require registration and processing of multisensor and multisource data, e.g., airborne radar, Thematic Mapper (TM), digital elevation models (DEM), and digital topographic data (roads, river networks, etc.). Although there are relatively few problems in rectifying TM data, the situation is more complex for airborne radar images, because the viewing geometry and the resulting image perturbations are more rapidly varying over the scene.

Various two-dimensional image transformations have been tested by different investigators for the radar case (Trevett, 1984). These transformations are fundamentally limited, in large scenes, by their inability to cope with local distortions such as those induced by relief. The results cited were between 5 and 100 metres as a function of the area size, the topography and the type of two-dimensional transformation used.

Also, stereo radar images enable a digital elevation model (DEM) and a digital radar map to be produced (Leberl *et al.*, 1986). Photographic products are created from the digital images and used in a photogrammetric stereo plotting instrument using a radargrammetric approach. Based on 16 check points, the random horizontal differences values were 30 metres in both directions (e.g., about 4 pixels of the SAR image used). Typically, an ortho-image may be generated with the DEM and auxiliary data from the stereo model measurements (Mercer, 1986).

In this paper, the method described is fully digital, including the SAR images, processing, and ortho-image generation. The model developed in this study uses a photogrammetric approach with the bundle adjustment technique based on the collinearity equations (Toutin, 1983). This rigorous model takes into account the physics of the viewing geometry (vector and sensor) and of the Earth (physical and dynamic).

Using ground control points (GCPs) and ancillary data, the bundle adjustment technique computes by least squares the parameters of the model, which allow the cartographic coordinates to be calculated from the image coordinates without iteration. Furthermore, this model enables stereoscopic radar images to be processed.

This geometric corrections model was originally developed for SPOT-HRV (Toutin, 1983; Toutin *et al.*, 1989), and was also tested on other data (Landsat-TM, MOS-MESSR, SEASAT-SAR) at the Canada Centre for Remote Sensing.

The purpose of this study is to extend the use of this model for airborne SAR data.

METHODOLOGY

RADAR IMAGING GEOMETRY

In the optical system, angles are the key to geometry; but for SAR, the phase is very important, and not the attitude. Assuming we know the zero time delay and the angle of zero Doppler, the SAR image is determined according to the time delay for the range direction, and to the Doppler frequency relative to the velocity vector of the aircraft for the azimuth direction.

Airborne SAR systems use motion compensation (hardware and software), which, although frequently excellent in geometric terms, may lead to small errors or residuals in azimuth image geometric precision. Normally, SAR motion compensation systems are constrained by requirements derived from the Doppler space. These requirements imply an along- track scale precision of less than a pixel over one frame, because the along-track pixel spacing is automatically controlled very accurately. There may occur skew distortion, however, and the impact of pitch combined with yaw, due to peculiarities of the CCRS implementation, may lead to zero Doppler error, then to geometric errors in azimuth (Raney, personal communication, 1991). In this paper, we assume the presence of such residuals and examine the effectiveness of their correction.

The slant range direction distortions in radar are about the same as those encountered in oblique photographic viewing. The radar perspective as it is represented in an image is portrayed as being orthogonal to the radar direction of illumination (Figure 1). Then, an incidence angle α of less than 90°, usually employed on SAR system, agrees with an equivalent angle $90° - \alpha$ for the oblique optical viewing (Raney, 1991). Therefore, the elevation displacement occurs in the "opposite direction." This relationship made, applicability of the SPOT case, or any other optical model becomes more apparent.

GEOMETRIC CORRECTION MODEL

The concept behind the geometric correction model is to generate a mathematical formulation of the geometry and residual motion of the radar system and of the environment. This model, then, is used with digital terrain data (GCPs, DEM) in order to

*Presently with Consultants TGIS Inc., 7667, curé Clermont, Anjou, Québec H1K 1X2, Canada

PHOTOGRAMMETRIC ENGINEERING & REMOTE SENSING,
Vol. 58, No. 4, April 1992, pp. 417–422.

0099-1112/92/5804–417$03.00/0

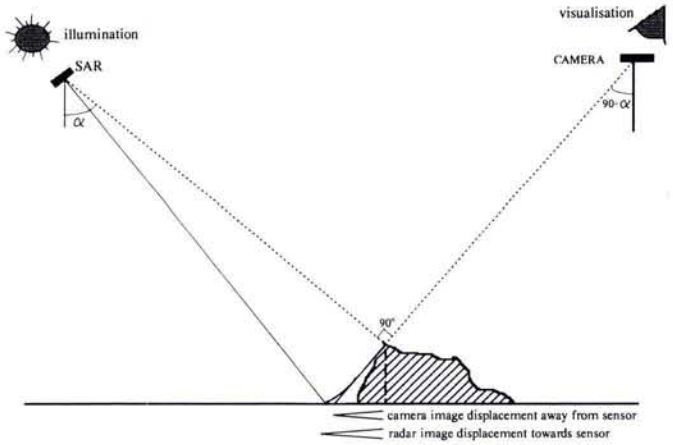

FIG. 1. Radar and camera image displacement.

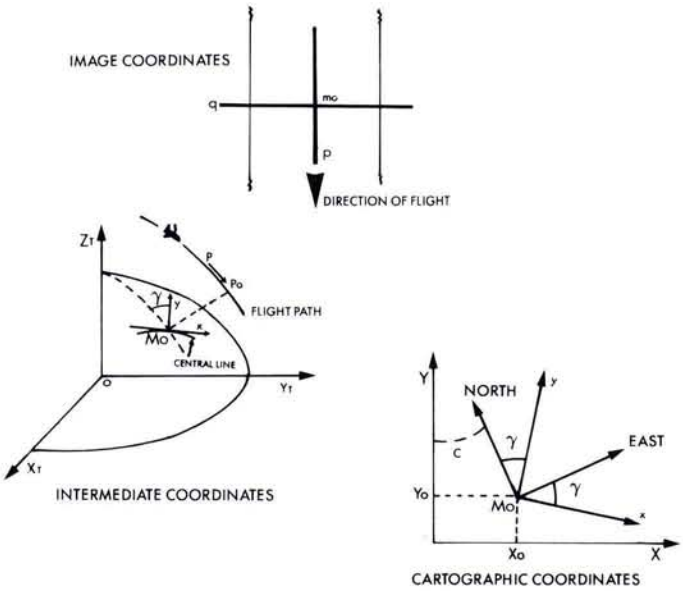

FIG. 2. Definition of coordinate systems.

give each pixel its true location in a cartographic system determined by the user.

This approach integrates together three different models: the motion, the sensor, and the Earth. Hence, the adjustment is simultaneous, taking into account the accuracy of each component. To develop this model, three coordinate systems are used (Figure 2):

- the image coordinates (m_o, p, q): centered on the central point of the image m_o, the p axis is the line coordinate, the q axis the pixel coordinates;
- the intermediate coordinates (M_o, x, y, h): centered on M_o, whose image position is m_o, the x axis being tangential to the ellipsoid in the central scan line plane; h is the elevation above the geoid;
- the coordinates (X, Y, Z) of the cartographic projection in which the rectification has to take place.

These three coordinate systems are used to subdivide the problem into sub-problems related to the cartographic system and the viewing geometry. Thus, the transformation between the intermediate and cartographic systems (two conformal cartographic projections) is simply reduced to a translation (X_o, Y_o) and a rotation (γ). We are then concerned only with the law of transformation between the image and intermediate systems.

For radar space resection, the collinearity equations are valid for three-dimensional Cartesian coordinates of a uniform reference system (Konecny *et al.*, 1986). The collinearity equation of a point P can be written in the instrumental reference system (P, x_t, y_t, z_t) linked to the instrument at time t, as follows:

$$x_t = 0$$
$$y_t + z_t \operatorname{tg}\beta = 0$$

in which β is the incidence angle at the point P,
x_t is the axis in the azimuth direction,
y_t is the axis in the across-track direction, and
z_t is the axis in the "altitude direction."

The process of changing from the instrumental reference system to the intermediate system may be broken down into a series of elementary transformations (Toutin, 1983):

(1) For the optical case, changing from the instrumental reference system to the orbital reference system by a rotation R integrating the pitch and the yaw. This transformation does not apply for the SAR case.
(2) Translation $-\rho = P0$ to arrive at a parallel reference system centered on 0, the Earth's center.
(3) Changing from the preceding reference system corresponding to the instant t, to a reference system corresponding to the instant $t = 0$ by a rotation $\mathbf{B}^{-1}$ which is a matrix developed as a function of time.
(4) Changing from the preceding reference system to a system in which the axis $0z$ goes through the central point M_0 of the scene through two rotations m_o and s_o, giving the matrix $\mathbf{M}$.
(5) Translation $r = 0M_o$ to center the new system in M_o.
(6) Exchange of axes x, y in $-y$, $+x$ to obtain axes in the conventional direction – matrix $\mathbf{K}$ – where
x = across-track direction;
y = displacement in time, the along-track direction.
(7) Changing from the preceding reference system to a reference system in which the y axis is in the meridian plane by a rotation $\mathbf{\Gamma}^{-1}$.
(8) Changing from the preceding reference system to a system in which the plane $M_o xy$ is tangential to the ellipsoid, and thus perpendicular to the normal, by a rotation Δ^{-1}.
(9) Passage from the preceding reference system to a system in which the x axis would be tangential to the scan path at the time $t = 0$ (terrestrial altitude 0) by a rotation $\mathbf{\Gamma}_o$.

In matrix form, the result is written

$$[x_t] = \mathbf{R}^{-1}\mathbf{B}\mathbf{M}\mathbf{K}^{-1}\mathbf{\Gamma}^{-1}\Delta^{-1}\mathbf{\Gamma}_0[x] + \mathbf{R}^{-1}\left\{\mathbf{B}\mathbf{M}\begin{bmatrix}0\\0\\r\end{bmatrix} - \begin{bmatrix}0\\0\\\rho+\delta_1\rho t\end{bmatrix}\right\}$$

The collinearity equations in the instrumental reference system are converted, using the elementary transformations described previously, into the collinearity equations in the intermediate system (x, y, h). The derivation of these equations is out of the scope of this paper; and as they are identical to the SPOT case, they can be found in Toutin (1983). Thus,

$$Pp + y(1 + \delta\gamma X) - \tau H = 0$$
$$X + \theta\frac{H}{\cos\chi} + \alpha q\left(Q + \theta X - \frac{H}{\cos\chi}\right) = 0$$

in which

$$X = (x - ay)\left(1 + \frac{h}{N_o}\right) + by^2 + cxy$$
$$H = h - \frac{x^2}{2N_o}$$

Each parameter is given by a mathematical formula (Toutin, 1986), which translates physical quantities of the viewing geometry (aircraft, Earth, geographic location of the scene).

P and Q	are the scale factors in Y and X, respectively;
τ and θ	are functions of the leveling angles in Y and X, respectively;
a	is a function of the skew;
H_o	is the aircraft altitude at the central viewing line;
N_o	is the normal to the ellipsoid;
$\chi, \delta\gamma, b, c$	are known parameters of the second order, functions of the geometry (aircraft, scene center, Earth center);
p and q	are the image coordinates; and
x, y, and h	are the ground coordinates in the intermediate system.

To the six uncorrelated unknowns (P, Q, θ, τ, a, b), three more must be added. These are related to the translation (X_o, Y_o) and rotation (γ) transformations previously described, necessary to pass to the cartographic coordinate system of the GCPs.

These equations can be written reciprocally as

$$y = v\,(1 - \delta\gamma u) + \tau H'$$

$$x = u\,(1 - \frac{h}{N_o}) + v(a - bv - cu) - \frac{H'}{\cos\chi}\,(\theta + \frac{1 + \theta^2}{Q}\,u)$$

in which

$$u = \frac{-\alpha q Q}{1 + \theta\alpha q}\,;\; v = -Pp\,;\; H' = h - \frac{u^2}{2N_o}.$$

The modeling of a scene is thus straight forward, and there are few unknowns (6 + 3). Each of these unknowns is in fact the combination of several correlated variables of the viewing geometry, so that the number of unknowns has been reduced to an independent set. Because of the term h in the equation for the altitude, it also allows stereoscopic views and homologous points (coplanarity equations) to be processed. Moreover, with modeling, the effect of each term can be determined in the reference system, through its development as a function of the flight, viewing, and Earth parameters. In summary, the features of this geometric corrections model to be noted are

- the integration of the different flight, viewing, and Earth parameters;
- the simplicity of its transformation equations; and
- the consideration of the flight path as an arc of ellipse "parallel to the Earth ellipsoid."

RESULTS

Test site

During early April 1987, a series of ice jams occurred in the Saint John River, New Brunswick, Canada, and its tributaries. In response to a need for information by the New Brunswick Department of Environment, the C/X airborne synthetic aperture radar system (C/X SAR) of the Canada Centre for Remote Sensing (CCRS) was flown over the lower Saint John River on 3 April 1987 to map the flood extent. A subset of the coverage, encompassing 25 kilometres of the river, was used to validate the geometric corrections model. The test area is presented on Figure 3.

The SAR image of the study area was acquired at C-band (5 GHz) and at horizontal-transmit horizontal-receive polarizations. The look direction was south, with incidence angles varying from 45° at the inner range to 76° at the far range. The representation is in ground range. The pixel size is 4 m by 5 m in azimuth and range directions, respectively. Aircraft altitude was approximately 6000 metres above ground level. Figure 4 is an example of the ground range image.

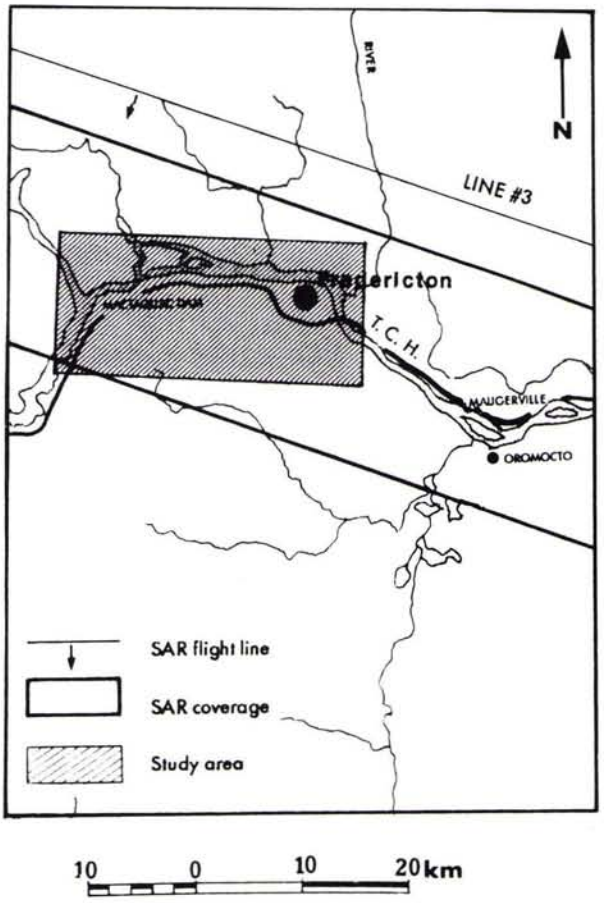

FIG. 3. SAR coverage and test area.

The test site is located in the vicinity of Fredericton, New Brunswick, and covers an area of approximately 20 x 18 square kilometers. Figure 5 shows a 1:50 000-scale topographic map of the site. The airborne SAR and the DEM coverage were considered to define the location and the size of the study area.

Digital Topographic Data

Description of the digital topographic data

The digital topographic data covering the test site consisted of positionally accurate digital maps at 1:10 000 scale. It was obtained from the Land Registration and Information Service, the Maritime provinces' mapping agency in Prince Edward Island. The supplied data were originally stereo-compiled from 1:35 000-scale aerial photographs.

The data were structured into a spatial database in a geographic information system (GIS) environment. The database contained a set of planimetric layers (roads, hydrography, landcover, etc., with a horizontal accuracy of 2.5 to 3.5 m) and an altimetric layer (DEM as a 25-m grid, with a vertical accuracy of 2.5 m). These data were used in their original projection (New Brunswick double stereographic) and reference system (ATS77*).

*ATS77 for Average Terrestrial System of 1977, refers both to the horizontal Datum (known as October 1977) and the ellipsoid used by the Maritime provinces mapping agency.

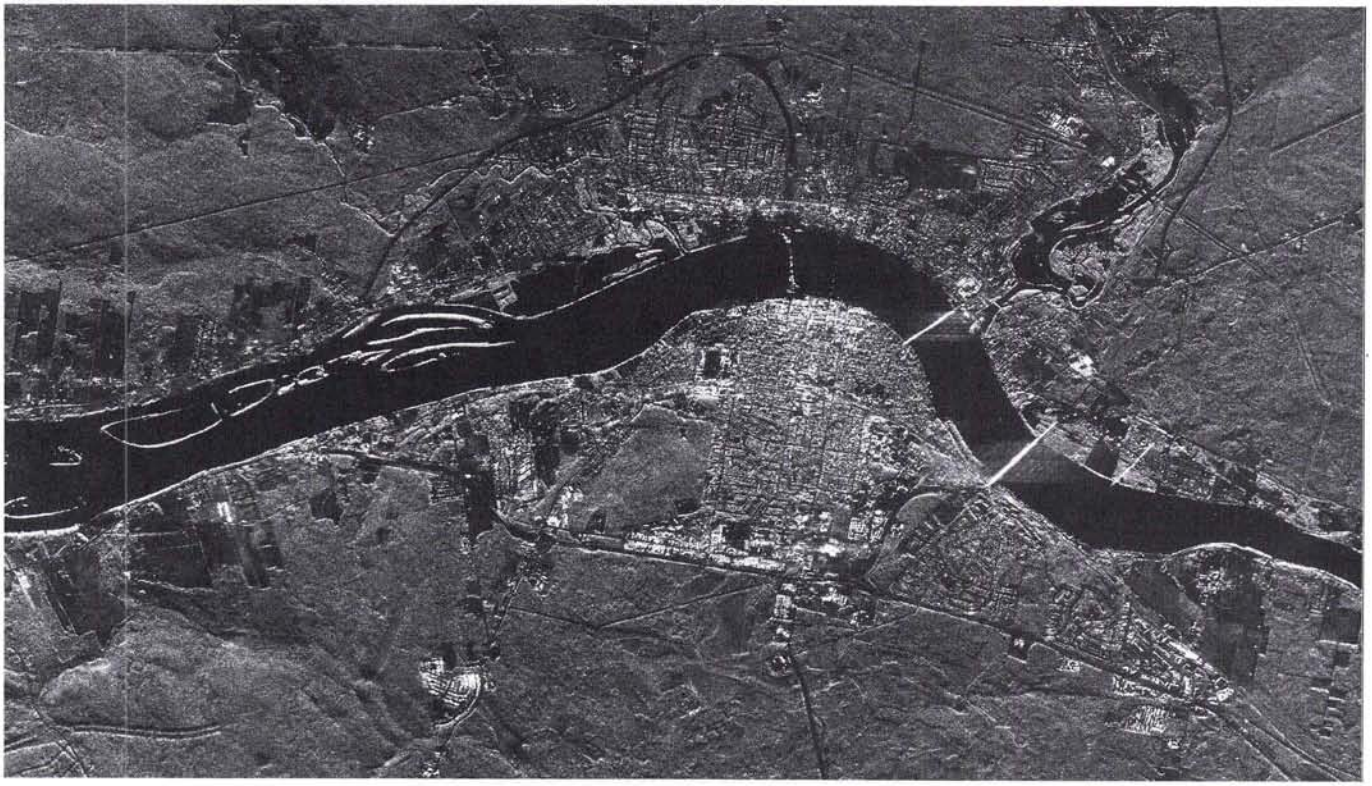

FIG. 4. Example of a portion of a ground range image.

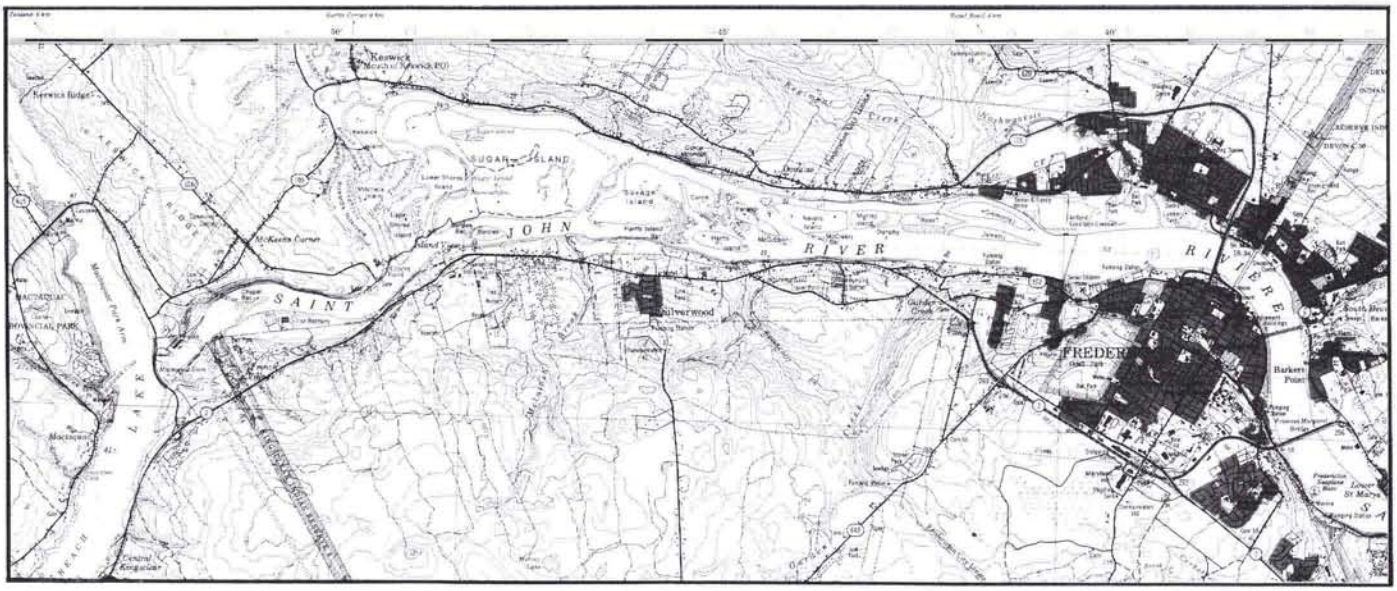

FIG. 5. NTS map sheet on the test site.

Acquisition of the control points

A set of control points (58) with an average plotting error of 2.5 pixels was manually identified on the radar imagery corresponding to road intersections with an image analysis system. For each of these points, their respective X,Y,Z values were obtained from the topographic database. Using the GIS functions, the elevation for each node was interpolated from the DEM. For this interpolation, the GIS software utilizes the inverse weighted distance nine-neighbor algorithm. Considering the range in elevation of the terrain, as described previously, the type of control points (i.e., road intersections) and the DEM grid size, the vertical accuracy of these control points is estimated to be within a ± 4-m range.

RESTITUTION ACCURACY

In order to verify the geometric model, a test was performed in which all the chosen control points were initially used. Starting with 58 GCPs in the model, 12 points were rejected, because

their residuals were more than 2.7 the root mean square of all the residuals, and are considered misplotted points. Thus, the residuals on the remaining 46 GCPs, given in Table 1, indicate the quality of the geometric modeling.

As the RMS residuals are on the order of 10 metres, these results mean that the mathematical formulation of the viewing geometry is a good fit to the physical reference and that the resulting error of the formulation can be neglected. Then, the main factor contributing to model accuracy (10 m) is the GCP image coordinate accuracy (10 to 12 m). Except for a few cases, the residuals are less than 20 metres (≈4 pixels).

In order to verify the quality of the restitution (errors on independent check points), different tests are performed using fewer points as GCPs in the model generation, and using the remaining data as independent check points. Figure 6 gives, for various configurations of GCPs (from 6 to 20), the RMS residuals in X and Y on the GCPs and the RMS errors on the check points (CPs). The former represents the accuracy of the model (as described previously), and the latter, the accuracy of the restitution and of the radar ortho-image generation.

Using between 8 and 15 GCPs, the RMS residuals on GCPs and the errors on CPs do not change significantly. The GCPs were generally distributed near the edge of the image to avoid extrapolation. When 20 GCPs were used, the errors on CPs decreased by about 10 percent. The main reason for this improvement is not the increase in the number but rather a better distribution of points in the middle of the image in the across-track direction, thus leading to a better computation in the least-squares adjustment of the range scale-factor.

In summary, we assert that using 10 GCPs, for this image size and geometry, a restitution accuracy (with respect to independent check points) of 11 m in X and 9 m in Y can be achieved.

Another way to verify this accuracy is to compare the resampled ortho-image (Figure 7, 25 by 11 km, pixel size of 6.25 m) with the road network of the digital topographical data. The cover of this issue of *PE&RS* gives a sub-image (5.6 by 5.6 km) as an example of this result. A qualitative viewing confirms the previous result of two pixels accuracy (10 to 12 m). But in some places, larger errors (5 pixels) are visible; and as they are local, further investigation should be made to find the source of discrepancies between the ortho-image and the road network. Of these, several are located along roads which are parallel to closely spaced contour lines. Because the main residual error is in the across-track direction, one can assume an error in the DEM creation from the contour lines in these areas during the resampling process.

TABLE 1. ROOT MEAN SQUARE (RMS) AND MAXIMUM RESIDUALS ON 46 GCPS

	RMS residuals (m)	Maximum residual (m)
X	11	19
Y	9	27

CONCLUSIONS

Comparisons with results obtained from other experiments are not necessarily meaningful as radar image and ground relief may differ considerably from one study to another. Our results seem to compare well with another fully digital methodology published earlier (Trevett, 1984) in the case of low relief. However, our model gives better results in medium and high relief and with a larger image (more than 10 by 10 km). Use of a DEM can be assumed to be responsible for the improved results.

One can also suggest that even though the proposed method is not yet fully developed for use in an operational environment, it appears that under favorable conditions, effective geometric corrections and rectification are feasible and may be expected to achieve, with 8 to 10 GCPs, an accuracy of 2 pixels with a good level of confidence.

Possible improvements in methodology include

(1) Improve the accuracy of GCP acquisitions to get better than 2 to 4 pixel errors, either by using a simulated image created with a DEM and correlation around the GCPs (Guindon, 1986, 1987); or by using reflecting targets like radar corner reflectors (Dowmann, 1984). In fact, the horizontal accuracy of ground points determined in radar images is depending mainly upon the quality of the ground points.

(2) Introduce the position record of the airborne motion to better fit arcs of ellipse which modeled the aircraft path.

(3) Introduce the flight path variations, because uncompensated across-track drift of the aircraft may cause azimuth-direction distortions (Blacknell, 1986).

(4) As for the optical case (Toutin, 1989), use two stereoscopic images from different paths to obtain an independent estimate of the third dimension. The stereoscopic plotting and processing will determine the altimetry and can improve the accuracy of cartographic mapping and point positioning (Gracie, 1970).

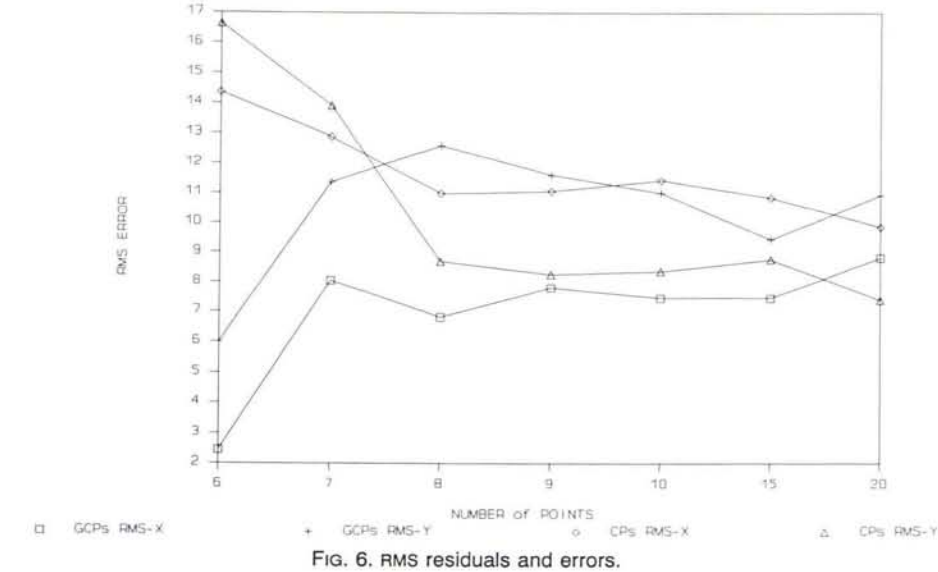

FIG. 6. RMS residuals and errors.

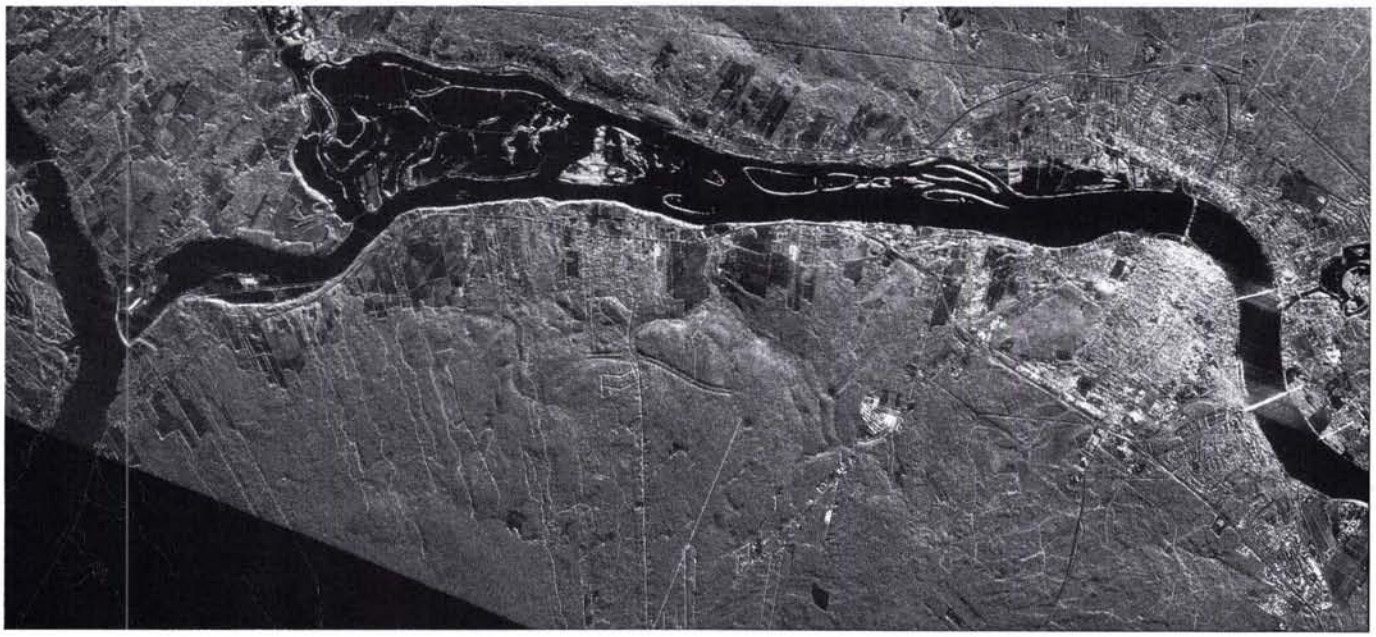

FIG. 7. Resampled SAR ortho-image (25 by 11 km).

(5) Transform the digital elevation model to a digital surface model by taking into account the forest height in the resampling process.

Under these conditions, there are strong reasons to believe that the same methodology, if applied on airborne SAR images with other viewing geometries, would be reliable for geometrically correcting images to a precision better than 2 pixels, with as few as 8 to 10 GCPs.

The acquisition of GCPs directly from the digital topographic source offers an advantage to this methodology. It can be implemented within the new generation of map image-processing systems which integrate raster and vector technologies. Registration of the imagery directly in the same coordinate system as the digital maps should facilitate the manipulation of the image-extracted information within the spatial database. Furthermore, the ortho-image which results from the correction process can be used directly as an additional layer in a spatial data base, in combination with other thematic, cartographic data to produce new cartographic products where the ancillary data overlays properly on the imagery.

ACKNOWLEDGMENTS

The authors wish to thank their colleagues Mr. Keith Raney and Mr. Robert Leconte at the Canada Centre for Remote Sensing for their scientific advice on SAR, Mr. Terry Pultz of Intera Technologies Inc., and Mr. Olivier Cochaux of the University of Quebec (Hull) for their professional assistance in the data acquisition.

REFERENCES

Blacknell, D., I.A. Ward, and A. Freeman, 1986. Motion compensation and geometric distortion in airborne SAR imagery, *Proceedings of the ISPRS Commission I Symposium*, 1-6 September 1986, Stuttgart, Germany, pp. 539–548.

Dowman, I.J., and R. Gibson, 1984. An evaluation of SAR-580 synthetic aperture radar for map revision and monitoring, *Proceedings of the SAR-580 Investigators Workshop*, May 1984, Ispra, Italy, pp. 195–213.

Gracie, G. *et al.*, 1970. *Stereo Radar Analysis*, Report No. FTR-1339-1, U. S. Engineer Topographic Laboratory, Ft. Belvoir, Virginia.

Guindon, B., 1987. Methods for automated control point acquisition in SAR images, *Proceedings of the First International Workshop on Image Rectification Techniques for Spaceborne Synthetic Aperture Radar*, January 1987, Loipersdorf, Austria, pp. 29–33.

Guindon, B., and H. Maruyama, 1986. Automated Matching of Real and Simulated SAR Imagery as a Tool for Ground Control Point Acquisition, *Canadian Journal of Remote Sensing*, Vol. 12, No. 4, pp. 149–158.

Konecny, G., and W. Schuhr, 1986. Introduction of geometric information to radar image data, *Proceedings of the ISPRS Commission I Symposium*, 1-5 September 1986, Stuttgart, Germany, pp. 141–147.

Leberl, F.W., G. Domik, and B. Mercer, 1987. Methods and Accuracy of Operational Digital Image Mapping with Aircraft SAR, *Proceedings of 1987 ASPRS-ACSM Annual Convention*, March- April 1987, Baltimore, Vol. 4, pp. 148–158.

Mercer, J.B., R.T. Lowry, F. Leberl, and G. Domik, 1986. Digital Terrain Mapping with STAR-1 SAR Data, *Proceedings of IGARSS '86 Symposium*, Zurich, Switzerland, pp. 645–650.

Toutin, Th., 1983. Analyse mathématique des possibilités cartographiques du satellite SPOT, *Mémoire du Diplôme d'Etudes Approfondies*, Ecole Nationale des Sciences Géodésiques, Institut Géographique National, Paris, France, pp. 1–74.

Toutin, Th., and Y. Carbonneau, 1989. La multi-stéréoscopie pour les corrections d'images SPOT, *Journal canadien de télédétection*, Vol. 15, No. 2, pp. 110–119.

Trevett, J.W. (ed.), 1984. *The European SAR-580 Experiment*, Investigator Final Report, Vol. 1, May 1984, Ispra, Italy, pp. 1–168.

(Received 8 May 1990; revised and accepted 23 April 1991)